HHS Public Access

Author manuscript

Clin Transl Imaging. Author manuscript; available in PMC 2018 October 01.

Published in final edited form as:

Clin Transl Imaging. 2017 October ; 5(5): 473–485. doi:10.1007/s40336-017-0245-8.

Biodistribution of 99mTc-MAA on SPECT/CT performed for 90Y radioembolization therapy planning: a pictorial review

JJ Bailey, **Y Dewaraja**, **D Hubers**, **RN Srinivasa**, and **KA Frey**

Department of Radiology, University of Michigan, 1500 E Medical Center Drive, Ann Arbor, MI 48103

Abstract

Purpose—To evaluate the frequency of 99mTc-MAA uptake in extrahepatic organs during 90Y radioembolization therapy planning.

Methods—This retrospective case series of 70 subjects who underwent 99mTc-MAA hepatic artery perfusion studies between January 2014 and July 2016 for 90Y radioembolization therapy planning at our institution involved direct image review for all subjects, with endpoints recorded: lung shunt fraction, extrahepatic radiotracer uptake, time from MAA injection to imaging.

Results—Combined planar and SPECT/CT imaging findings in the 70 subjects demonstrated lung shunt fraction measurements of less than 10% in 53 (76%) subjects and greater than 10% in 17 (24%) subjects. All patients demonstrated renal cortical uptake, 23 (33%) demonstrated salivary gland uptake, 23 (33%) demonstrated thyroid uptake, and 32 (46%) demonstrated gastric mucosal uptake, with significant overlap between these groups. The range of elapsed times between MAA injection and initial imaging was 41–138 min, with a mean of 92 min. There was no correlation between time to imaging and the presence of extrahepatic radiotracer uptake at any site.

Conclusions—During hepatic artery perfusion scanning for 90Y radioembolization therapy planning, extrahepatic uptake is common, particularly in the kidney, salivary gland, thyroid and

Corresponding Author: Jason J. Bailey, MD, jasonjamesbailey@gmail.com, Phone: 862-432-5173, Fax: 734-936-8182.

Conflict of Interest: JJ Bailey, Y Dewaraja, D Hubers, R Srinivasa, and KA Frey declare that they have no conflict of interest.

Compliance with Ethics Guidelines:

1. No author has any conflict of interest, including Jason Bailey, Yuni Dewaraja, David Hubers, Ravi Srinivasa, and Kirk Frey.
2. This study was performed with IRB approval with waiver of informed consent and conformity to the Declaration of Helsinki.

Author contributions:

JJ Bailey: Literature search, Literature review, Writing, Editing, Content planning, Data collection and management, Protocol/project development

Y Dewaraja: Literature review, editing, content planning, protocol/project development, data analysis

D Hubers: Literature review, editing, protocol/project development

R Srinivasa: Literature review, editing, content planning, protocol/project development

KA Frey: Literature search, Literature review, Editing, Content planning, Data collection and management, Protocol/project development

gastric mucosa, and is hypothesized to result from breakdown of 99mTc-MAA over time. Given the breakdown to smaller aggregates and ultimately pertechnetate, this should not be a contraindication to actual Y-90 microsphere therapy. Although we found no correlation between time to imaging and extrahepatic uptake, most of our injection to imaging times were relatively short.

Keywords

Hepatic artery perfusion sctinigraphy; Y90 radioembolization; Biodistribution; Macroaggregated albumin Body:

Patients with hepatocellular carcinoma have several different locoregional treatment options including thermal ablation, transarterial chemoembolization, radioembolization and stereotactic body radiation therapy (SBRT). Those patients with multifocal hepatocellular carcinoma are often treated with ^{90}Y radioembolization therapy for palliation as larger volumes of tumor can be treated in staged sessions. The main limitation to ^{90}Y radioembolization, however, is hepatopulmonary shunting of radiotracer and subsequent pulmonary injury. To avoid this complication, pre-procedural planning using ^{99m}Tc-MAA is performed and lung shunt fractions are calculated, with ^{90}Y dosage adjusted accordingly or radioembolization avoided entirely [1].

Traditionally, estimates of pulmonary radiotracer uptake and the lung shunt fraction relative to hepatic uptake are calculated based on planar imaging. With increasing availability of SPECT/CT, however, and the possibility of potentially dangerous extrahepatic, extrapulmonary localizations of radioemboli, an increasing number of institutions now acquire both planar and SPECT/CT images during ^{99m}Tc-MAA hepatic artery perfusion studies for ^{90}Y radioembolization planning [2–5]. As a result, both potentially dangerous and benign extrahepatic localizations of radiotracer are identified more frequently during treatment planning, and the interpreting physician must be ready to distinguish between such findings.

At our institution, reconstitution of ^{99m}Tc-MAA kits follows manufacturer guidelines (Jubilant DraxImage) and at the end of synthesis we perform elution testing with thin layer chromatography daily to evaluate the radiochemical purity of all ^{99m}Tc-MAA used that day, with an average of 97% purity for routine production in our facility. Reconstituted kits are used within 6 hours and radiochemical purity remains stable prior to injection. The protocol for hepatic artery perfusion studies involves cannulation of the hepatic arterial system in the interventional radiology suite, subsequent injection of ^{99m}Tc-MAA into a branch of the hepatic artery, transfer to immediate post-procedural observation, and subsequent imaging in the nuclear medicine department.

We performed a retrospective review of 70 cases of ^{99m}Tc-MAA hepatic artery perfusion studies between January 2014 and July 2016 for ^{90}Y radioembolization therapy planning at our institution. Direct image review of each study was performed, with the following endpoints recorded: lung shunt fraction (from anterior abdominal and posterior thoracic planar images); other locations of extrahepatic radiotracer uptake (from planar head and neck images, lower thorax-upper abdominal SPECT/CT images); and time from MAA

injection to imaging. Patterns of ^{99m}Tc-MAA uptake outside of the liver and lung are summarized in Table I. Lung shunt fraction measurements of less than 10% were seen in 53 (76%) subjects, from 10–15% in 11 (16%) subjects, from 15–20% in 3 (4%) subjects, and greater than 20% in 3 (4%) subjects. Twenty-three subjects (33%) demonstrated salivary gland uptake and 23 (33%) demonstrated thyroid uptake, with 21 of these subjects overlapping (21/25; 84%). Gastric mucosal uptake was seen in 32 (46%) subjects, with 22 of these subjects also demonstrating either salivary or thyroid uptake (22/32; 69%). Renal cortical uptake of variable intensity was demonstrated in all 70 subjects. Other less frequently observed regions of uptake included the spleen (4 subjects; 6%), the paraumbilical vein (4 subjects; 6%), bowel (1 subject; 1%), and heart (1 subject; 1%). The range of elapsed times between MAA injection and initial imaging was 41–138 min, with a mean of 92 min. There was no correlation between time to imaging and the presence of extrahepatic radiotracer uptake at any site.

Radiotracer uptake in the salivary glands, thyroid gland, and gastric mucosa (Figs 1, 8, & 10) usually coexisted and were frequently seen after ^{99m}Tc-MAA injection. This does not reflect direct shunting of MAA from the hepatic artery [2–5]. This distribution pattern is characteristic of free pertechnetate, and is most likely a result of ^{99m}Tc-MAA breakdown in vivo [3]. Salivary gland and thyroid gland uptakes are clearly related to such indirect physiology [2]. Supporting this hypothesis is the fact that there is generally some delay between radiotracer injection in the interventional radiology suite and eventual imaging in the nuclear medicine department [3,4]. This is unlike, for example, intravenous ^{99m}Tc-MAA injection for pulmonary perfusion scanning. This is not associated with an incidental “pertechnetate” distribution of radiotracer in our laboratory, likely because of the very short interval between injection and imaging. It is important to note that pertechnetate uptake in the gastric mucosa is readily distinguishable from MAA delivered directly to the wall of the stomach on SPECT/CT imaging. The former is characterized by diffuse gastric activity, sparing the serosal surfaces of the stomach. Conversely, direct access of injected MAA to the gastric artery can arise during hepatic arterial injections, and is characterized by regional (usually lesser curvature) activity extending from the serosal to the mucosal surfaces on SPECT/CT. Such tracer delivery may lead to debilitating gastric ulceration as a complication of ^{90}Y therapy [5].

Renal cortex retention of radiotracer was seen in virtually all patients during ^{90}Y planning, and is of variable intensity (Fig 6 & 7). Renal cortex activity is seen even more frequently than the pertechnetate-like distribution of salivary glands, thyroid gland and gastric mucosa, suggesting that it occurs either by a separate pathway or earlier in the breakdown of ^{99m}Tc-MAA than generation of free pertechnetate. We hypothesize that intermediate proteolytic breakdown products of ^{99m}Tc-MAA, resulting in smaller albumin aggregates, can pass hepatic and pulmonary capillary beds, but become lodged in the glomerulus. Such renal uptake of radiotracer should not be considered a contraindication to subsequent ^{90}Y therapy.

A diffuse pattern of radiotracer uptake can also be identified rarely in the spleen (Fig 3). This could be related to inadvertent reflux of ^{99m}Tc-MAA into the splenic artery during injection, especially given that the injection of ^{99m}Tc-MAA is generally less selective within the hepatic arterial system than actual ^{90}Y injection. Another possibility is that splenic

uptake is similar to renal cortical uptake and relates to the breakdown of MAA into smaller particles that are eventually filtered by the reticuloendothelial system. This is not a contraindication to radioembolization.

Radiotracer uptake can be seen occasionally also in a recanalized paraumbilical vein of cirrhotic patients with portal hypertension (Figs 4 & 9). The physiology underlying this finding is unclear. Cirrhosis and portal hypertension resulting in recanalization of the portal vein result in blood being shunted away from the resistant portal vasculature and into the systemic circulation. A possible explanation for recanalized paraumbilical vein uptake is that flow in this vessel is very slow and turbulent in some patients, resulting in a physical lag in local blood pooling. Another possibility is that as the MAA gradually breaks down in the liver over time, rather than proceeding antegrade into the hepatic venous drainage. Portal hypertension may cause some of the particles to flow steadily into the recanalized paraumbilical vein even hours after injection. Yet another explanation could be the presence of tumor thrombus in the recanalized paraumbilical vein.

Potentially deleterious sites of radiotracer uptake identified during hepatic artery perfusion scanning can, of course, also be identified, and this is a primary purpose of the ^{99m}Tc-MAA planning study. Lung uptake itself (Fig 3), characterized as the percentage of radiotracer shunting to the lungs compared to the liver, is traditionally the dose limiting factor for ^{90}Y treatment because it reflects the likelihood of radiation pneumonitis and fibrosis. The likelihood of treatment success, however, is based on tumor dosimetry, not percentage of lung shunting [6]. SPECT/CT allows more accurate calculation of dosimetry to the hepatic tumor itself. This means that even if the lung shunt fraction is elevated and ^{90}Y dose must be decreased, the actual dosimetry to the hepatic tumor may still be therapeutic and patients previously thought to be ineligible for radioembolization might be able to receive beneficial radioembolization at a lower administered dose.

The gallbladder can receive perfusion from the hepatic circulation and can be difficult or impossible to identify separately from the liver on planar imaging alone (Fig 5). If ^{90}Y is deposited in the gallbladder wall, radiation-induced cholecystitis can occur. The gallbladder, however, is a relatively radioresistant organ. Although somewhat controversial, precautionary measures are generally not required when low-level gallbladder uptake is seen during treatment planning. Cases with a significant concentration of ^{99m} Tc-MAA in the gallbladder wall might benefit from cystic artery embolization, percutaneous cholecystostomy or cholecystectomy as pre-therapeutic precautionary measures.

A rare but potentially startling site of radiotracer uptake is the heart (Fig 2). Uptake in the myocardium can be seen on SPECT/CT, but is unlikely to relate to direct delivery from hepatic arteries. Instead, uptake seen in the heart is more likely related to particulate ^{99m}Tc-MAA breakdown, however, in at least one instance (Fig 2), the observed activity appears associated with the ventricular blood pool. Therapeutic ^{90}Y-microemboli are not expected to follow this pattern of distribution, and apparent cardiac uptake in therapy planning should not prevent patients from radioembolization eligibility.

To improve study quality and reduce radiotracer distribution and intensity in extrahepatic organs, it has been suggested that ^{99m}Tc-MAA injection-to-imaging time should be kept as low as possible, preferably less than 1 hour. It has also been reported that lengthy times from injection to imaging can increase the lung shunt fraction, which could result in eligible patients being excluded from the potential benefits of radioembolization [3–4].

Optimal treatment planning and utilization of hepatic artery radioembolic therapy requires differentiation of contraindicated patterns of direct hepatic arterial tracer delivery from patterns of radiotracer deposition associated with in vivo breakdown of ^{99m}Tc-MAA rather than radioemboli. Image misinterpretation could result in damage to a critical organ or to unnecessary rejection of patients who might benefit from radioembolization.

References

1. Garin E, Rolland Y, Laffront S, Edeline J. Clinical impact of 99mTc-MAA SPECT/CT-based dosimetry in the radioembolization of liver malignancies with 90Y-loaded microspheres. Eur J Nucl Med Mol Imaging. 2016; 43:559–575. [PubMed: 26338177]
2. Lee RGL, Hill TC, Rolla AP, Clouse ME. Re: Thyroid Activity on Technetium-99m Macroaggregated Albumin Lung Scans. J Nucl Med. 1983; 24:749–750. [PubMed: 6223991]
3. De Gersem R, Maleux G, Vanbilloen H, Baete K, Verslype C, Haustermans K, Verbruggen A, Van Cutsem E, Deroose CM. Influence of time delay on the estimated lung shunt fraction on 99mTc-labeled MAA scintigraphy for 90Y microsphere treatment planning. Clin Nucl Med. 2013 Dec; 38(12):940–2. [PubMed: 24212439]
4. Uliel L, Royal HD, Darcy MD, Zuckerman DA, Sharma A, Saad NE. From the angio suite to the gamma-camera: vascular mapping and 99mTc-MAA hepatic perfusion imaging before liver radioembolization-a comprehensive pictorial review. J Nucl Med. 2012 Nov; 53(11):1736–47. [PubMed: 23124868]
5. Lenoir L, Edeline J, Rolland Y, Pracht M, Raoul JL, Ardisson V, Bourquet P, Clement B, Boucher E, Garin E. Usefulness and pitfalls of MAA SPECT/CT in identifying digestive extrahepatic uptake when planning liver radioembolization. Eur J Nucl Med Mol Imaging. 2012 May; 39(5):872–80. [PubMed: 22237844]
6. Blau M, Wicks R, Thomas SR, Lathrop KA. Radiation absorbed dose from albumin microspheres labeled with technetium-99m. Task Group of the Medical Internal Radiation Dose Committee. The Society of Nuclear Medicine. J Nucl Med. 1982 Oct; 23(10):915–7. [PubMed: 6214620]
7. Prince JF, van den Hoven AF, van den Bosch MA, Elschot M, de John HW, Lam MG. Radiation-induced cholecystitis after hepatic radioembolization: do we need to take precautionary measures? J Vasc Interv Radiol. 2014; 25(11):1717–23. [PubMed: 25442134]
8. Giammarile F, Bodei L, Chiesa C, Flux G, Forrer F, Kraeber-Bodere F, Brans B, Lambert B, Konijnenberg M, Borson-Chazot F, Tennvall J, Luster M. Therapy, Oncology, and Dosimetry Committees. EANM procedure guideline for the treatment of liver cancer and liver metastases with intra-arterial radioactive compounds. Eur J Nucl Med Mol Imaging. 2011 Jul; 38(7):1393–406. DOI: 10.1007/s00259-011-1812-2 [PubMed: 21494856]

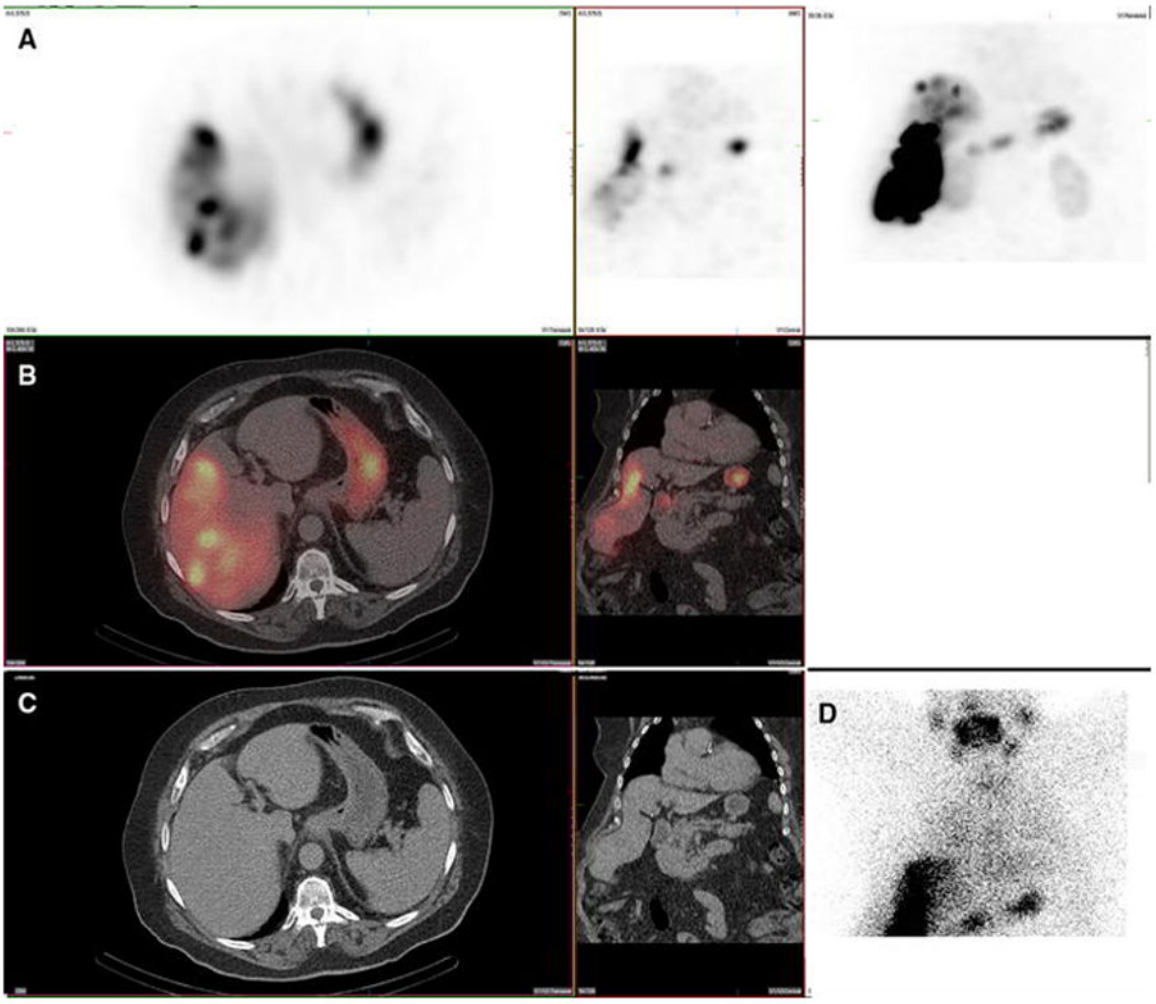

Figure 1. Gastric mucosa. Also present: salivary, thyroid, kidney

A 67-year-old male with hepatocellular carcinoma and no prior radioembolization was administered ^{99m}Tc-MAA via right groin access into the right hepatic artery and imaged 75 minutes after injection. Calculated lung shunt fraction was 14%. He underwent ^{90}Y-radioembolization 15 days later without complication.

Axial, coronal, and MIP SPECT (Row A); Axial and coronal fused SPECT/CT (Row B); Axial and coronal CT (Row C); and anterior planar (D) images demonstrate radiotracer uptake in the gastric mucosa. Note that the surrounding gastric serosal wall is spared, suggesting this is not related to an accessory artery arising from the hepatic vasculature. Expected radiotracer uptake is also seen in the right hepatic lobe tumor. Anterior planar images demonstrate uptake in the gastric mucosa as well as uptake in the salivary glands and thyroid gland. Note that gastric activity is uniform and diffuse, and spares the serosal gastric surface. Radiotracer uptake in the kidney (not shown) was also present. This uptake pattern, including gastric mucosa, salivary glands, and thyroid gland, is typical of free pertechnetate, and likely relates to in vivo breakdown of ^{99m}Tc-MAA.

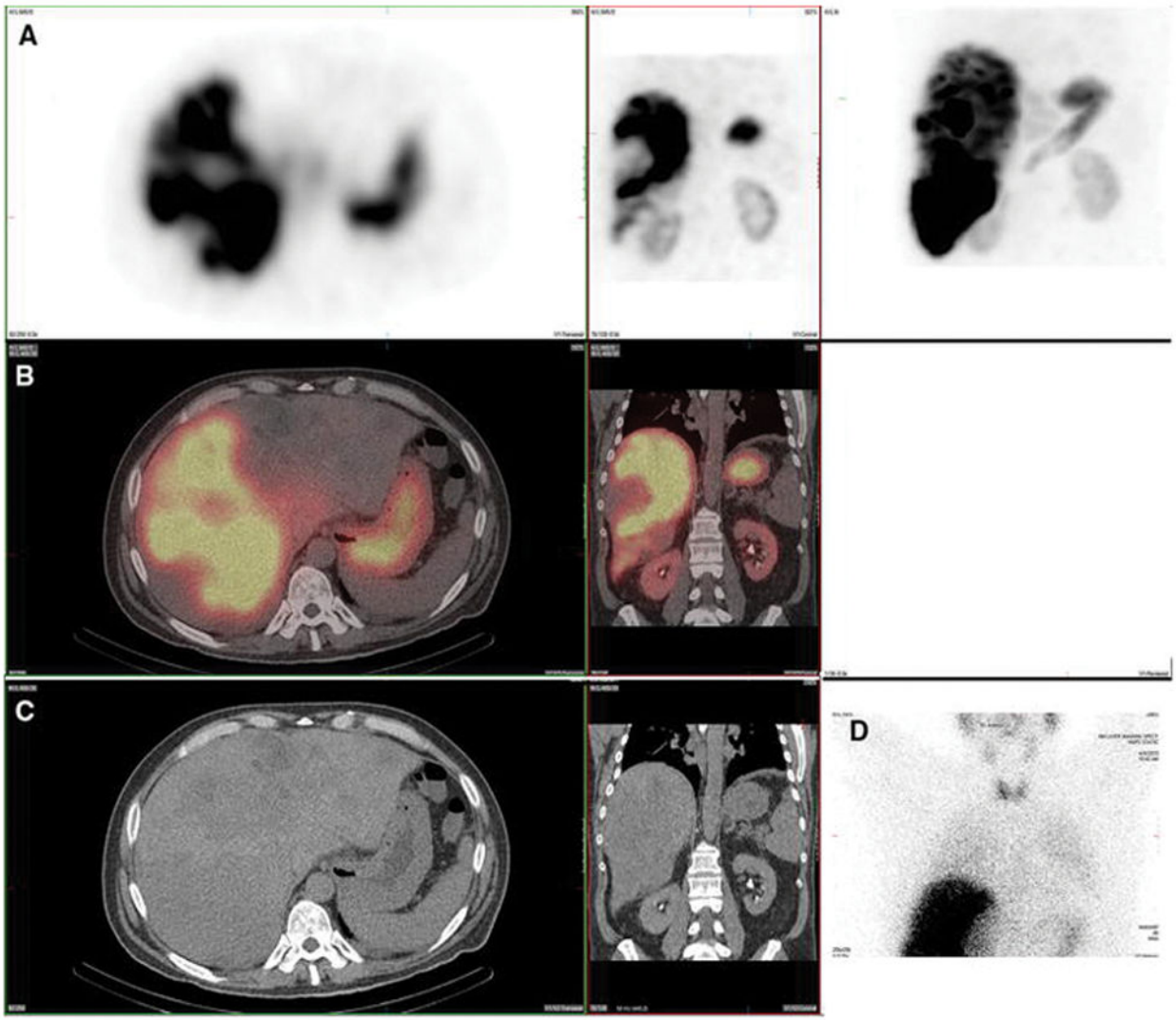

Figure 2. Heart. Also present: stomach, thyroid, kidney, spleen

A 57-year-old male with metastatic colon adenocarcinoma and no prior radioembolization was injected with ^{99m}Tc-MAA via right groin access into the right posterior hepatic artery and imaged 96 minutes after injection. Calculated lung shunt fraction was 17%. He did not undergo subsequent ^{90}Y-radioembolization.

Axial, coronal, and MIP SPECT (Row A), axial and coronal fused SPECT/CT (Row B), axial and coronal CT (Row C), and anterior planar (D) images demonstrate radiotracer uptake in the heart, possibly related to cardiac blood pool. Anterior planar and MIP images also demonstrate radiotracer uptake in the thyroid gland, stomach, and kidney. Radiotracer uptake in the spleen (not shown) was also present.

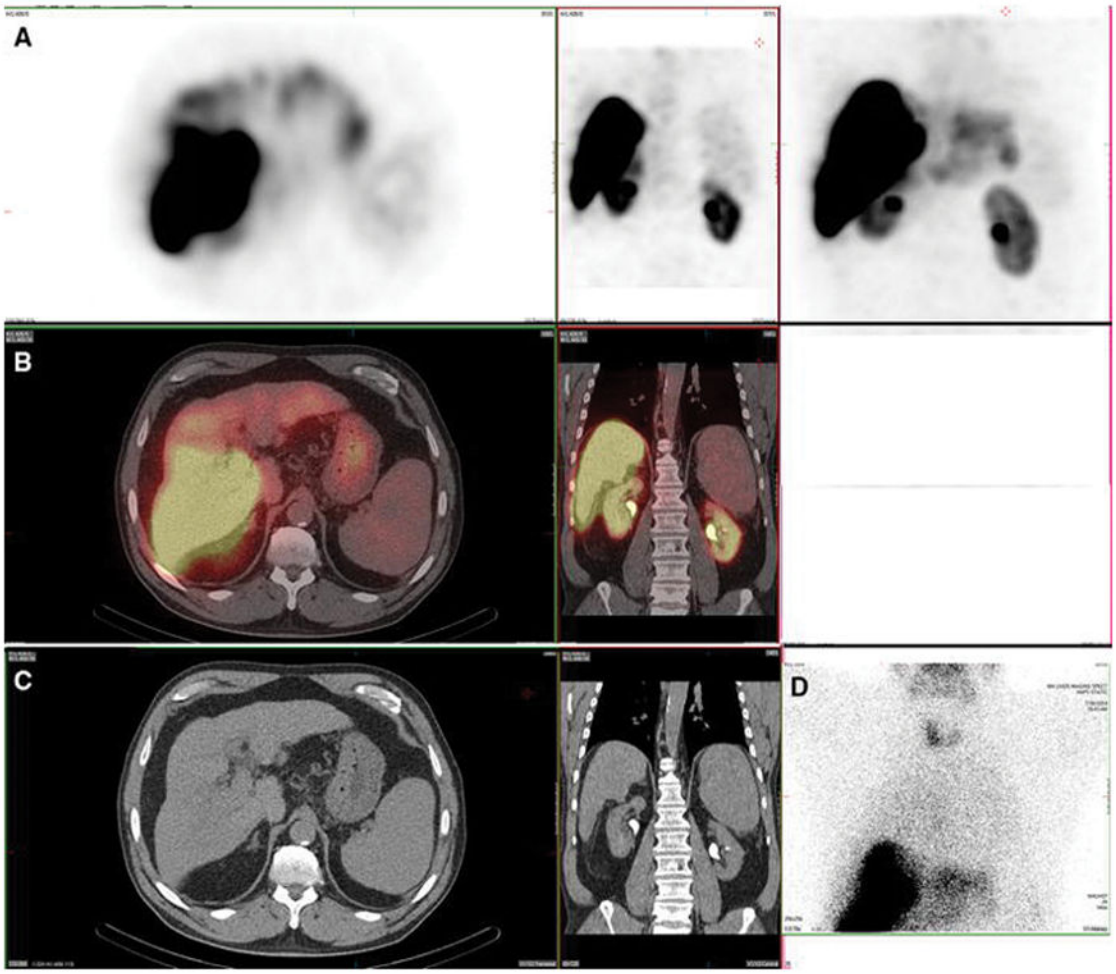

Figure 3. Lung and spleen. Also present: salivary glands, thyroid, kidney, stomach and heart

A 61-year-old female with metastatic neuroendocrine cancer, carcinoid syndrome, and no prior radioembolization, was injected with ^{99m}Tc-MAA via right groin access into the right hepatic artery and imaged 73 minutes after injection. Calculated lung shunt fraction was 26%. She did not undergo subsequent ^{90}Y-radioembolization.

Axial, coronal, and MIP SPECT (Row A), axial and coronal fused SPECT/CT (Row B), axial and coronal CT (Row C), and anterior planar (D) images demonstrate radiotracer uptake in the lungs, consistent with hepatopulmonary shunting. The lung shunt fraction in this case was 26%, and ^{9} Y radioembolization was not performed. Radiotracer uptake was also seen in the renal cortices, which is a common site of extrahepatic uptake of radiotracer during hepatic artery perfusion studies, and is hypothesized to relate to breakdown of ^{99m}Tc-MAA over time, with lodging of smaller aggregates in renal capillaries. Anterior planar and MIP images also demonstrate radiotracer uptake in the salivary glands, thyroid gland, and stomach, consistent with the distribution of free pertechnetate.

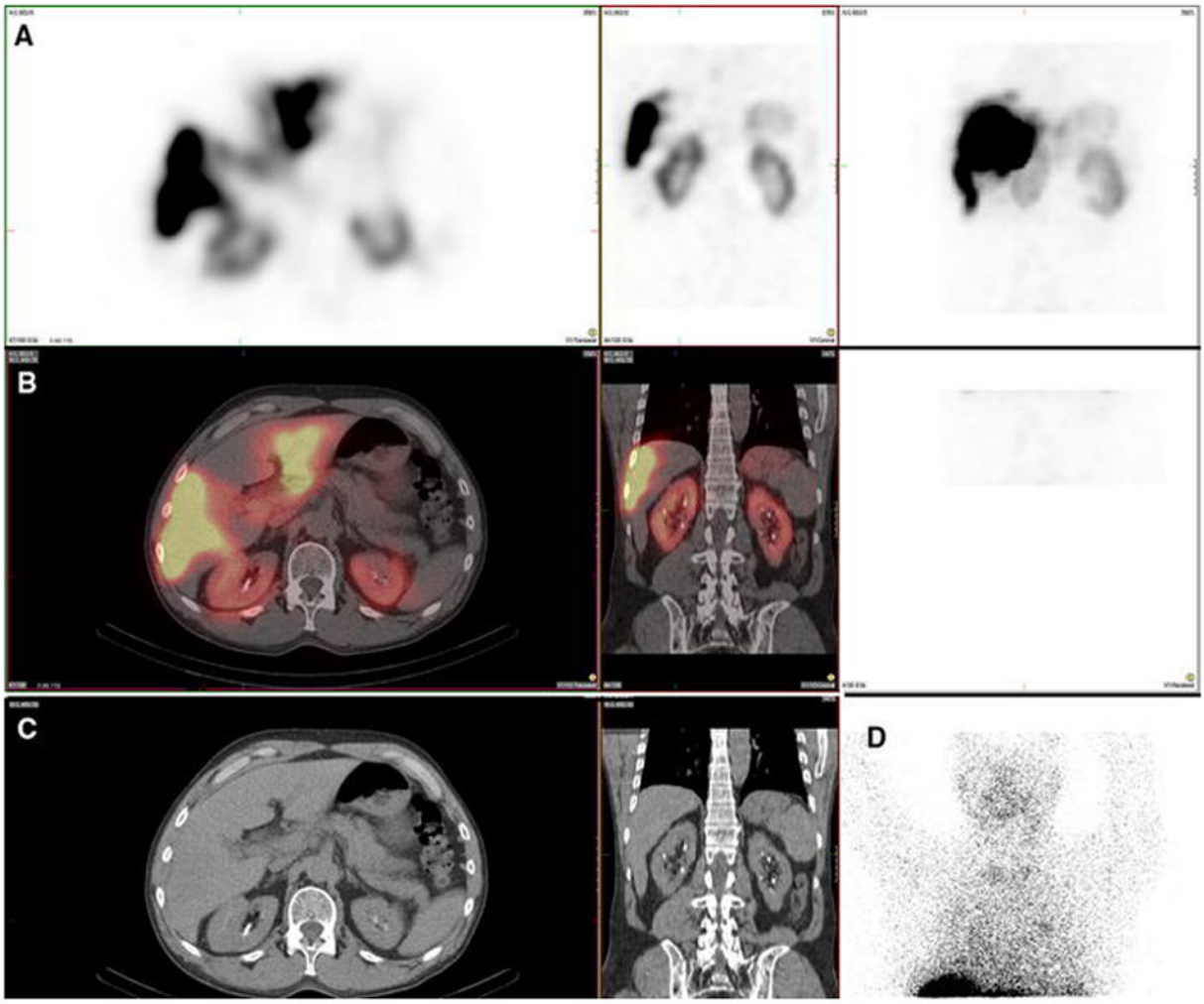

Figure 4. Recanalized paraumbilical vein. Also present: kidney, salivary glands, thyroid, stomach

A 62-year-old male with hepatocellular carcinoma and no prior radioembolization was injected with ^{99m}Tc-MAA via right groin access into the left hepatic artery and imaged 70 minutes after injection, with calculated lung shunt fraction of 5%. He underwent ^{90}Y-radioembolization 27 days later without complication.

Axial, coronal, and MIP SPECT (Row A), axial and coronal fused SPECT/CT (Row B), axial and coronal CT (Row C), and anterior planar (D) images demonstrate radiotracer uptake in a recanalized paraumbilical vein in this patient with underlying cirrhosis and portal hypertension. Anterior planar images also demonstrate radiotracer uptake in the salivary glands and thyroid gland. Radiotracer uptake in the stomach and kidneys (not shown) was also present.

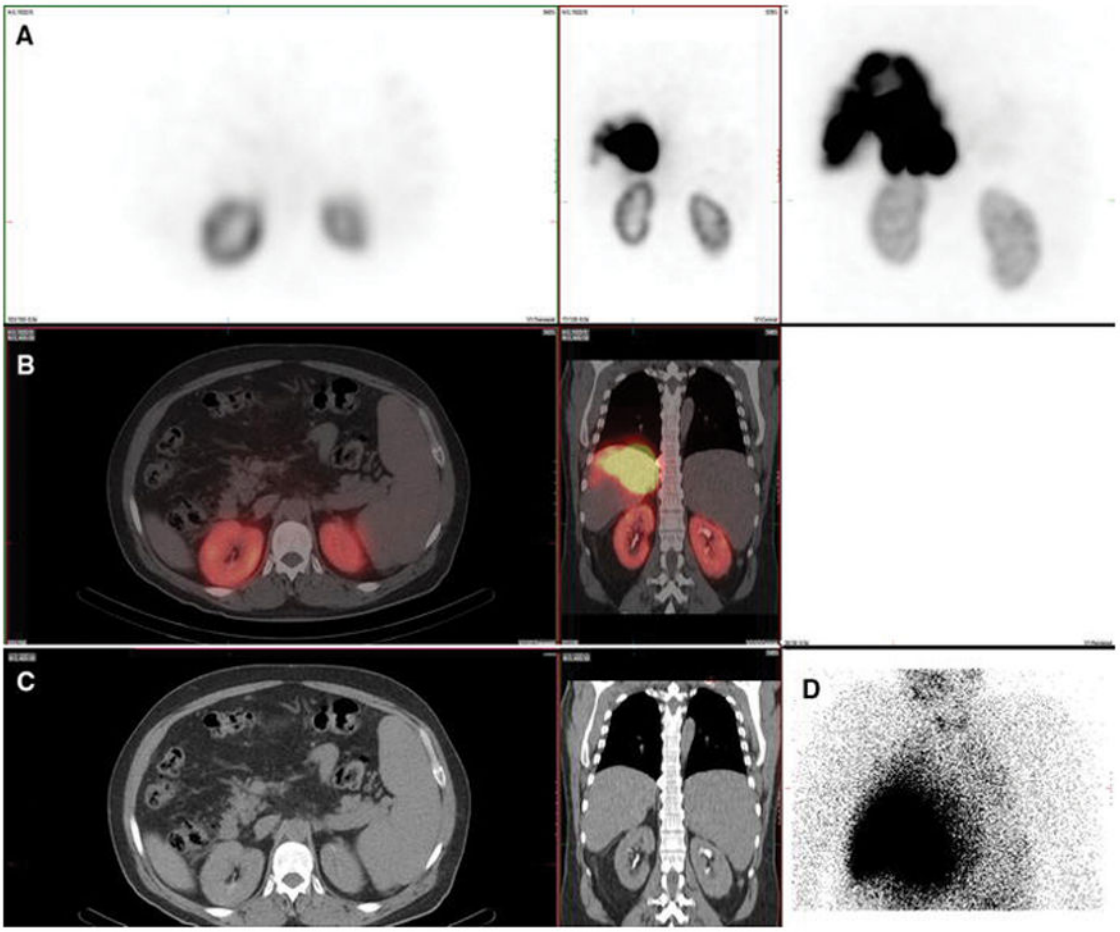

Figure 5. Gallbladder wall. Also present: salivary glands, thyroid, stomach, kidney

A 63-year-old male with hepatocellular carcinoma and no prior radioembolization was injected with ^{99m}Tc-MAA via right groin access into the replaced right hepatic artery and imaged 79 minutes after injection. Calculated lung shunt fraction was 13%. He did not undergo ^{90}Y-radioembolization because of prominent gallbladder activity.

Axial, coronal, and MIP SPECT (Row A), axial and coronal fused SPECT/CT (Row B), axial and coronal CT (Row C), and anterior planar (Fig D) images demonstrate radiotracer uptake in the gallbladder wall. Although controversial, low-level uptake in the gallbladder may not pose significant risk of gallbladder injury, given that it is relatively radio-resistant. When marked uptake is observed, such as this case, radioembolization is often avoided. There is also expected radiotracer uptake in the hepatic tumor. Anterior planar and MIP images also demonstrate radiotracer uptake in the stomach and kidney. Radiotracer uptake in the salivary glands and thyroid gland (not shown) was also present.

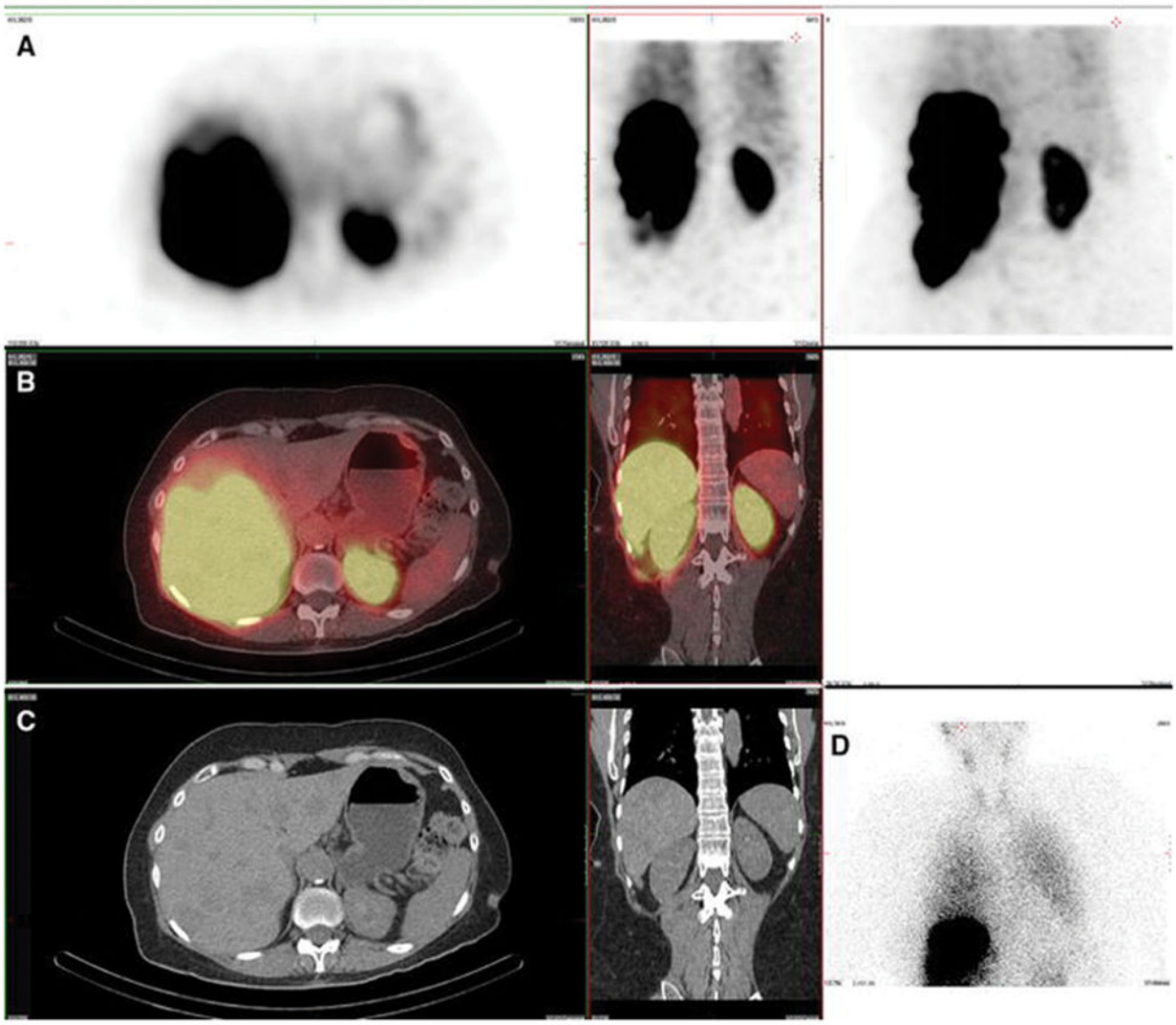

Figure 6. Kidney. Also present: salivary, gastric, thyroid

A 60-year-old male with hepatocellular carcinoma and no prior radioembolization was injected with ^{99m}Tc-MAA via right groin access into both the right and left hepatic arteries and imaged 131 minutes after injection. Calculated lung shunt fraction was 6%. He underwent ^{90}Y-radioembolization 15 days later without complication.

Axial, coronal, and MIP SPECT (Row A), axial and coronal fused SPECT/CT (Row B), axial and coronal CT (Row C), and anterior planar (D) images demonstrate radiotracer uptake in the renal parenchyma in a symmetric, bilateral distribution. This is hypothesized to relate to proteolytic breakdown of MAA into smaller aggregates that may pass hepatic and pulmonary capillaries, but lodged in renal glomeruli. There is also expected radiotracer uptake in the hepatic tumor as well as in the gastric mucosa. Anterior planar images also demonstrate radiotracer uptake in the salivary glands and thyroid gland.

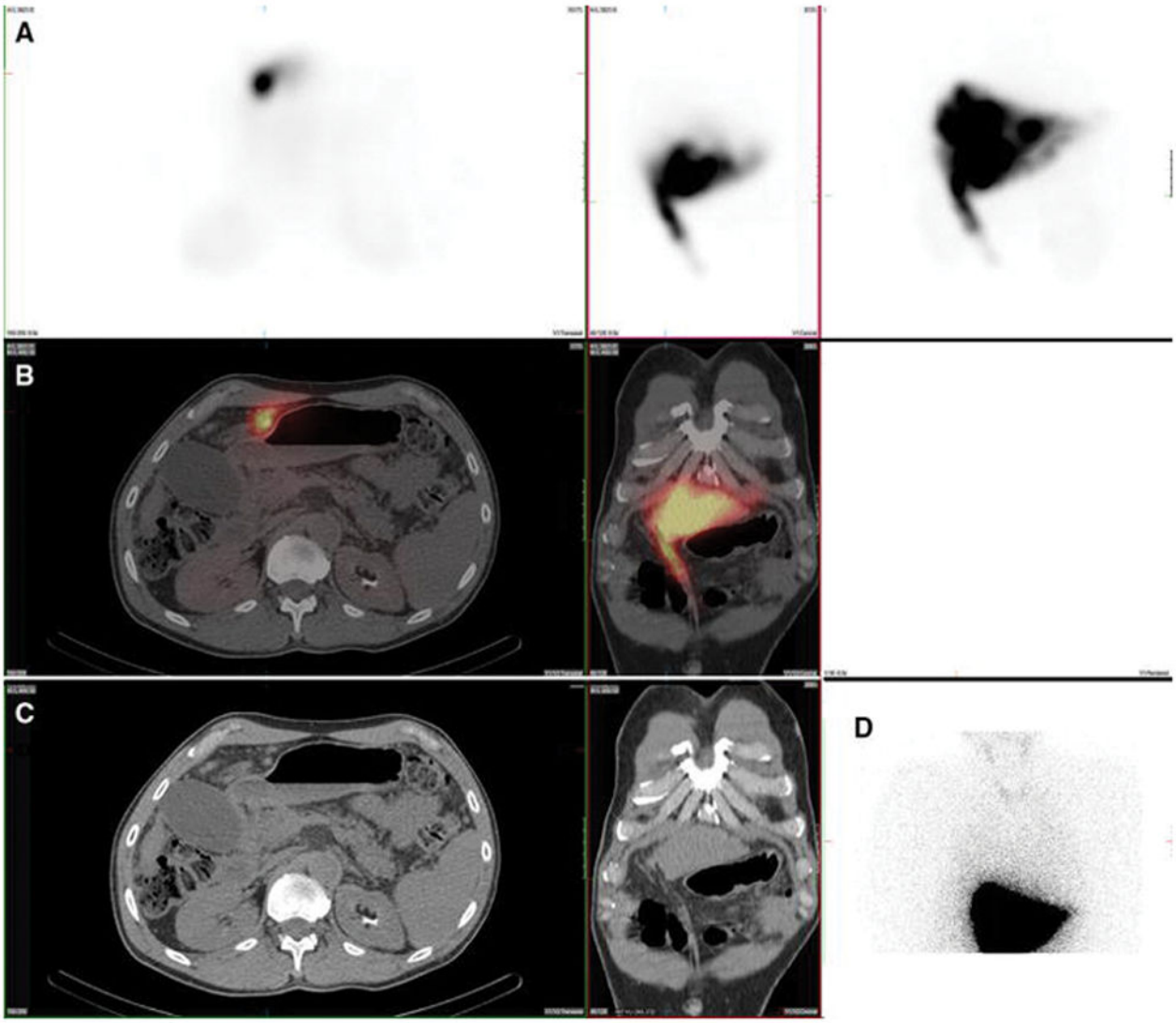

Figure 7. Kidney

A 59-year-old male with hepatocellular carcinoma and no prior radioembolization was injected with ^{99m}Tc-MAA via right groin access into the right hepatic artery and imaged 126 minutes after injection. Calculated lung shunt fraction was 3%. He underwent ^{90}Y-radioembolization 20 days later without complication.

Axial, coronal, and MIP SPECT (Row A), axial and coronal fused SPECT/CT (Row B), axial and coronal CT (Row C), and anterior planar (D) images demonstrate radiotracer uptake in the renal parenchyma, likely related to MAA breakdown over time. Renal cortical uptake, of variable intensity, was the most commonly seen location of extrahepatic radiotracer uptake on hepatic artery perfusion studies, seen in 100% of cases. Note that radiotracer is not seen in the renal collecting system, and thus, activity is not due to excretion into the urinary tract.

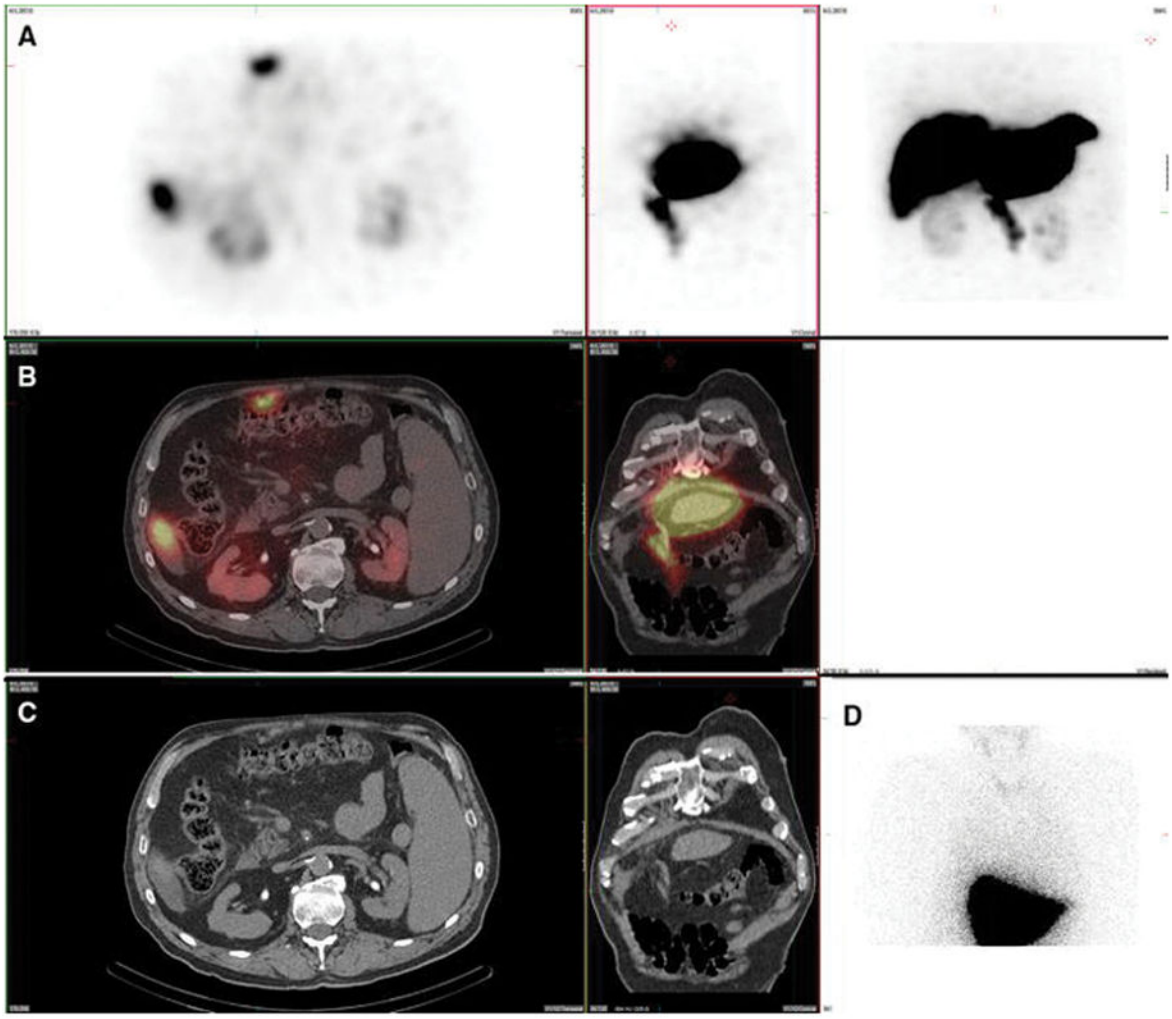

Figure 8. Gastric mucosa. Also present: salivary glands, thyroid, kidneys

A 63-year-old male with metastatic neuroendocrine carcinoma and no prior radioembolization was injected with ^{99m}Tc-MAA via right groin access into the right hepatic artery and imaged 107 minutes after injection. Calculated lung shunt fraction was 8%. He underwent ^{90}Y-radioembolization 21 days later without complication.

Axial, coronal, and MIP SPECT (Row A), axial and coronal fused SPECT/CT (Row B), axial and coronal CT (Row C), and anterior planar (D) images demonstrate radiotracer uptake throughout the gastric mucosa, but not in the gastric serosa, consistent with a pertechnetate distribution. Corresponding uptake in the salivary glands and thyroid gland is seen on the anterior planar image. Uptake was also seen in the kidney.

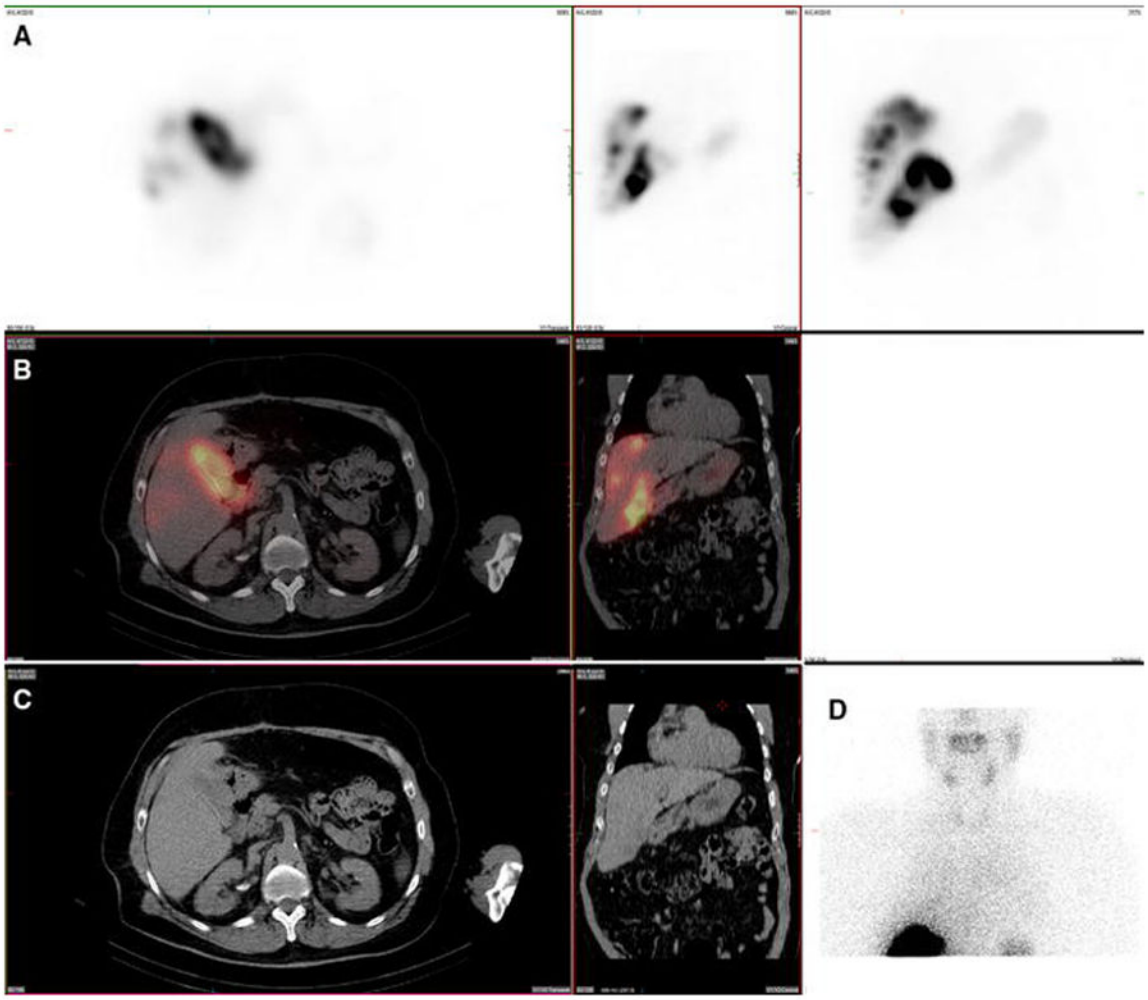

Figure 9. Paraumbilical vein. Also present: kidney

A 78-year-old male with cirrhosis, portal hypertension, and intrahepatic cholangiocarcinoma with mixed a hepatocellular carcinoma component and no prior radioembolization was injected with ^{99m}Tc-MAA via right groin access into both right and left hepatic arteries. He had prior preventative embolization occlusion of a falciform artery arising from the left hepatic artery, and was imaged 108 minutes after injection. Calculated lung shunt fraction was 3%. He underwent ^{90}Y-radioembolization 27 days later without complication.

Axial, coronal, and MIP SPECT (Row A), axial and coronal fused SPECT/CT (Row B), axial and coronal CT (Row C), and anterior planar (D) images demonstrate radiotracer uptake within a recanalized paraumbilical vein, extending along the inferior surface of the liver and continuing in the anterior right portion of the abdomen. This finding becomes apparent in cases of cirrhosis with portal hypertension, which are not uncommon during hepatic artery perfusion scintigraphy, given the associated prevalence of hepatocellular carcinoma within this patient population. Uptake was also seen in the kidney.

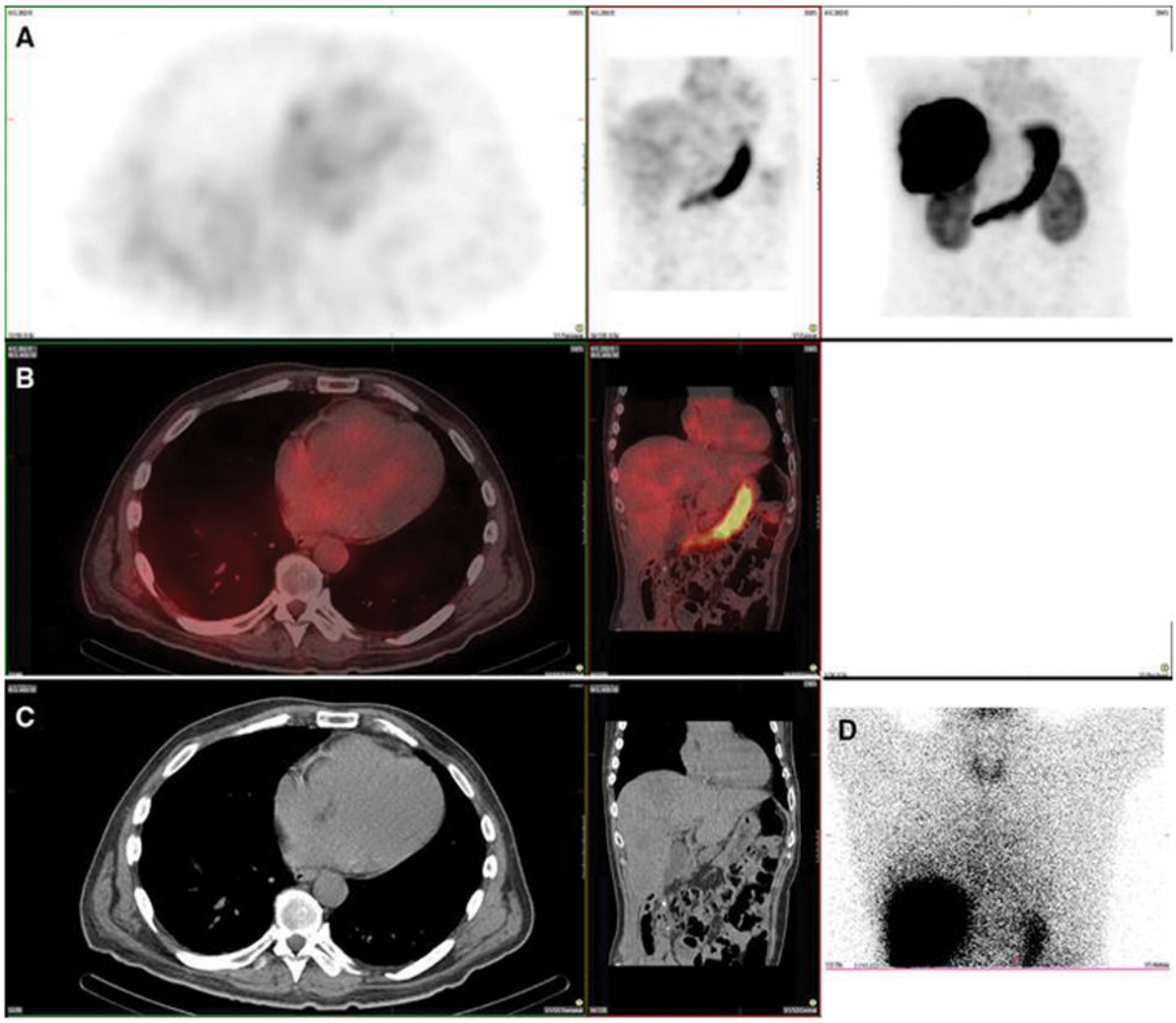

Figure 10. Gastric mucosa. Also present: Thyroid, salivary glands, kidney

A 78-year-old male with hepatocellular carcinoma and no prior radioembolization was injected with ^{99m}Tc-MAA via right groin access into the right hepatic artery and was imaged 109 minutes after injection. Calculated lung shunt fraction was 16%. He did not undergo ^{90}Y-radioembolization because of extensive portal venous thrombus identified during angiography.

Axial, coronal, and MIP SPECT (Row A), axial and coronal fused SPECT/CT (Row B), axial and coronal CT (Row C), and anterior planar (D) images demonstrate radiotracer uptake within the gastric mucosa and not the serosa, as well as in the thyroid and salivary glands, consistent with a pertechnetate distribution. This case also demonstrates radiotracer uptake in the spleen, which, similar to but less commonly seen than the renal cortex, is hypothesized to relate to proteolytic breakdown of MAA into smaller aggregates, which may be subsequently cleared by the reticuloendotheliar system.

Table I

Distribution of extrahepatic uptake of 99mTc-MAA (n = 70)

Lung Shunt Fraction	
• < 10%	53 (76%)
• 10–15%	11 (16%)
• 15–20%	3 (4%)
• > 20%	3 (4%)
Salivary Glands	23 (33%)
Thyroid Gland	23 (33%)
Both Salivary and Thyroid Gland	21 (30%)[a]
Gastric Mucosa	32 (46%)
Gastric Mucosa and either Salivary or Thyroid Gland	22 (31%) [b]
Renal Cortex	70 (100%)
Spleen	4 (6%)
Paraumbilical Vein	4 (6%)
Bowel	1 (1%)
Myocardium	1 (1%)

[a]21 of the total 70 patients demonstrated simultaneous salivary and thyroid gland uptake. Thus, 21 of the 25 (84%) patients with either salivary gland or thyroid gland uptake also demonstrated uptake in the other gland.

[b]22 of the total 70 patients demonstrated simultaneous gastric mucosal and either salivary gland or thyroid gland uptake. Thus, 22 of the 32 (69%) patients with gastric mucosal uptake also demonstrated either salivary gland or thyroid gland uptake.